American Mineralogist, Volume 88, pages 301–307, 2003

Equation of state of stishovite to lower mantle pressures

DENIS ANDRAULT,[1,*] ROSS J. ANGEL,[2] JED L. MOSENFELDER,[3] AND TRISTAN LE BIHAN[4]

[1]Laboratoire des Géomatériaux, Institut de Physique du Globe, Université Paris 7, Paris, France
[2]Crystallography Laboratory, Department of Geological Sciences, Virginia Tech, Blacksburg, Virginia 24060, U.S.A.
[3]Department of Geological and Planetary Sciences, California Institute of Technology, Pasadena, California 91125, U.S.A.
[4]European Synchrotron Radiation Facility, BP 200, F-38043 Grenoble, France

ABSTRACT

We performed new diffraction experiments to clarify the equation of state (EoS) of stishovite after we suspected systematic errors in previous experimental reports. Using diamond anvil cells, we repeated both single-crystal X-ray diffraction measurements under hydrostatic conditions and powder diffraction measurements using the laser-annealing technique and NaCl pressure medium. The major improvement is the increase in precision of the pressure determination using the quartz and NaCl equations of state. Using both sets of data, the stishovite bulk moduli were refined to K_0 = 309.9(1.1) GPa and K_0' = 4.59(0.23). We also reinvestigated the mechanism of the phase transformation to the $CaCl_2$-structured polymorph of SiO_2 at about 60 GPa. We confirm no volume discontinuity at the transition pressure, but the $CaCl_2$ form appears slightly more compressible than the rutile-structured form of SiO_2. This change in compression behavior is used for quantitative analyses of the spontaneous strains of the pressure-induced phase transition.

INTRODUCTION

The availability of very bright, third-generation synchrotron sources provides an ideal tool to measure unit-cell volumes from micrometer-sized samples at high pressures. The major remaining experimental challenges to determining reliable equations of state (EoS) up to extremely high pressures are the achievement and measurement of hydrostatic pressure. Quasi-hydrostatic pressures up to more than 100 GPa can be produced in the diamond anvil cell (DAC) using very soft pressure media such as He or Ne (Jephcoat et al. 1986). Another solution entails using harder pressure media (e.g., NaCl) and then relaxing the stresses at very high temperatures by annealing with an IR laser (Andrault and Fiquet 2001). Using the laser heating technique, energy barriers between high-pressure polymorphs can also be overcome more easily. Very high pressures are also easier to generate with hard media rather than He or Ne, which often induce failure of the diamond anvils. At moderate pressures, below the crystallization pressure (at about 12 GPa) of the water-alcohol-methanol mixture commonly used in DAC experiments, generating perfectly hydrostatic pressures is much easier.

Measuring pressure in the diamond-anvil cell requires the use of a secondary pressure standard. The most commonly used pressure standard is the fluorescence line of ruby, which has been calibrated against the equations of state (EoS values) of various metals, in turn derived from shock-wave experiments (Mao et al. 1978, 1986). The precision of the metallic EoS values is questionable, because they are derived from experiments performed at the simultaneous high pressures and temperatures generated along Hugoniot curves. Therefore, recent experiments have been devoted to the aim of determining an absolute pressure calibration based on simultaneous measurements of sound speeds and X-ray diffraction on standard materials. At the current time there are no such experimental data of sufficient precision available to significantly improve the accuracy of the common secondary pressure scales, although such results are imminent. An intermediate approach was pursued by Angel et al. (1997). They determined the EoS of quartz by single-crystal X-ray diffraction, using a pressure scale derived from the ruby calibration. The agreement of the bulk modulus determined from these measurements with that obtained from bench-top ultrasonic determinations of the elastic tensor of quartz (McSkimmin et al. 1965) indicates that the ruby pressure scale is accurate to within 0.3% to 10 GPa. Another problem arising from the use of metals as pressure standards is the poor precision obtained for the pressure measurement as a result of their relatively high bulk moduli. The use of a softer pressure standard increases the precision, because a given accuracy in the volume measurement corresponds to a smaller pressure error.

In a previous study, we reported the stishovite EoS up to 120 GPa, and a phase transition to the $CaCl_2$ distortion pressure at about 60 GPa (Andrault et al. 1998). Those data indicated that the phase transformation does not significantly affect the compression curve. The EoS was constrained by two types of diffraction experiments, performed at moderate pressures on a single crystal (Ross et al. 1990), and up to the highest pressures on powders. Both types of experiments could be improved. The experiments at higher pressures were performed without any pressure medium, using Pt as a pressure marker.

* E-mail: andrault@ipgp.jussieu.fr

Other experiments we have performed since that time have led us to suspect systematic errors in the pressures determined using the Pt EoS reported by Jamieson et al. (1982). Therefore, we performed new powder diffraction experiments at the ID30 beamline of ESRF, again using the laser-annealing technique that is required to relax stresses at extreme pressures, but this time using NaCl as a pressure medium. We determined pressure using both the ruby-fluorescence technique and the EoS of the B1- and B2-forms of NaCl. These data were supplemented by single crystal X-ray diffraction data collected up to 10 GPa, using the quartz EoS to determine pressure.

Experimental procedure

Single crystal diffraction

Single-crystal X-ray diffraction measurements were performed at the Bayerisches Geoinstitut (BGI) with a stishovite crystal synthesized from Corning grade G silica glass in a multi-anvil experiment at 14 GPa and 1300 °C for 10 hours. The crystal was loaded in water-alcohol-methanol mixture into a diamond-anvil cell (Allan et al. 1996) along with a quartz crystal for pressure measurement and a crystal of coesite. Diffraction measurements were performed with a customized Huber four-circle diffractometer. The unit-cell parameters of all crystals were obtained by a vector-least-squares fit of the diffractometer setting angles of low-angle strong reflections determined by the Single software (Angel et al. 2001a). Additional experimental details are reported elsewhere (Angel et al. 2001b). Between 9 and 11 stishovite reflections, and 9 and 12 reflections from the quartz crystal were used at each pressure.

Powder diffraction

X-ray powder diffraction was carried out in the angle-dispersive mode at the ID30 beamline of the ESRF (Grenoble, France). A channel-cut, water-cooled monochromator was used to produce a bright, monochromatic X-ray beam at 0.3738 or 0.4126 Å wavelength. Vertical and horizontal focusing were achieved by bent-silicon Pt-coated mirrors, the curvature of which were optimized to obtain an optimal X-ray flux at a full width at half maximum (FWHM) 12 × 15 μm spot on the sample. Two-dimensional images were recorded on an imaging plate, and refined in Lebail and Rietveld modes using the general structure analysis program package GSAS (Larson and Von Dreele 1988). More experimental details can be found elsewhere (Andrault and Fiquet 2001; Fiquet and Andrault 1999).

We used a diamond anvil cell with a large optical aperture, equipped with diamond anvils with 300 μm diameter culets. Rhenium gaskets were pre-indented to a thickness of ~40 μm and drilled to a diameter of 80 μm. The SiO_2 sample consisted of a pre-packed pellet of a mixture of SiO_2 glass and Pt, embedded between two pellets of NaCl. Besides providing an accurate pressure measurement using the EoS of the B1 (Brown 1999) or B2 form of NaCl (Sata et al. 2002), NaCl ensures hydrostatic pressure conditions and thermal insulation between the sample and diamonds. We did not insert ruby chips into the pressure chamber, to avoid chemical reaction with the SiO_2 sample during the high-temperature annealing.

The use of IR lasers enables the in situ synthesis of stishovite. We used a power stabilized multimode YAG laser, directed at the sample using a simple optical lens located at a distance of 25–30 mm from the sample. With this arrangement we could achieve hot spots greater than 40 μm in diameter. An optical microscope was used to scan the laser over the entire sample, and the temperature was estimated from the color of the sample to be 2300 ± 200 K. The FWHM of the X-ray diffraction lines did not increase with pressure, indicating that stresses could be optimally relaxed at all pressures.

We present a typical diffraction image and its 2Θ integration for a sample consisting of a mixture of NaCl, Pt, and stishovite (Fig. 1). Diffraction rings appear slightly spotty as a result of the high-temperature annealing step, which promotes

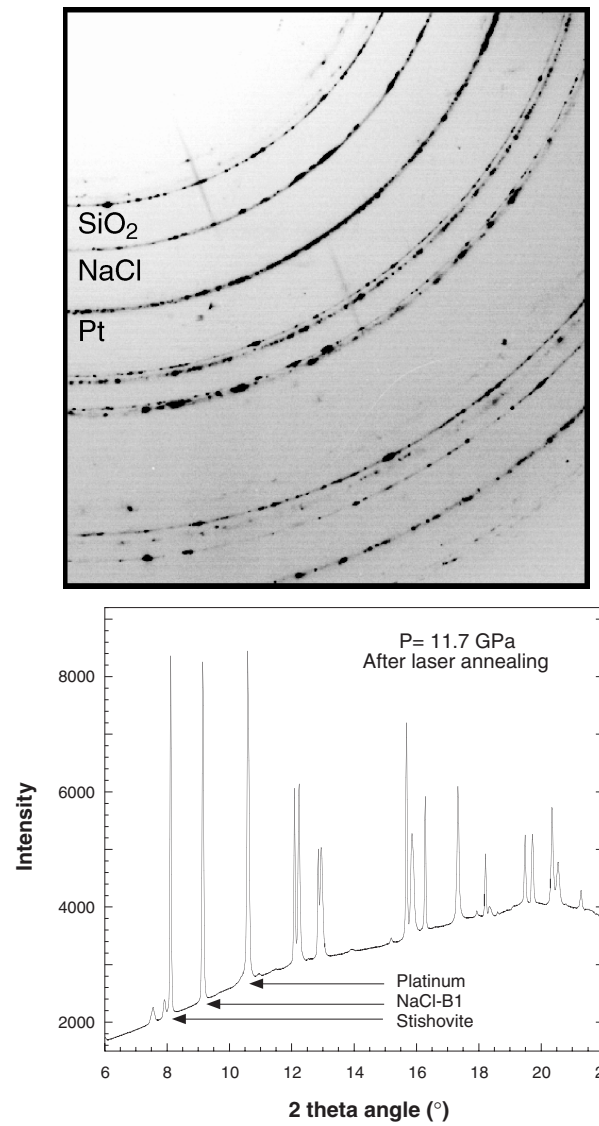

Figure 1. X-ray diffraction image (**a**) and its 2θ integration (**b**) recorded from a mixture of NaCl, SiO_2, and Pt powder in the diamond anvil cell at ≈12 GPa. The stishovite crystals were synthesized in situ during IR-laser heating at 2300(200) K, using Pt as an absorber of the YAG-laser. NaCl provides both a pressure medium and a pressure standard.

grain growth. Nevertheless, the rings remain very clear, indicating that the number of grains is sufficiently large to allow accurate unit-cell refinements.

Experimental accuracy and precision

All EoS's reported here were determined by a least-squares fit of the observed pressures to the measured volumes by v5.2 of the EosFit program (Angel 2001). We report the parameters for the Birch-Murnaghan finite-strain formulism throughout, but no significant differences are obtained if the Vinet EoS is used instead. Weights for each data point in the least-squares fits were derived from the estimated uncertainties in both pressure and volume via the effective variance method (Orear 1982) as implemented in EosFit.

For the single-crystal data the unit-cell volume of quartz was used to determine the pressure through its equation of state (Angel et al. 1997). Quartz provides a pressure standard consistent with the ruby scale and it yields a typical reproducibility in pressure measurement of ~0.01 GPa up to 10 GPa. Extensive studies have shown that the standard deviations of the volumes obtained from the single-crystal measurements are also reasonable estimates of their reproducibility. Therefore the standard deviations of the stishovite volumes have been used in fitting the stishovite EoS together with pressure uncertainties derived from the uncertainty in the corresponding quartz volume.

For powder diffraction data, pressure is derived from the measured NaCl volume using the associated EoS's for the B1 or B2 forms. The accuracy of the NaCl volume determination is converted into an experimental precision for the pressure determination of ~0.3% at 10 GPa in the B1 phase, and ~0.2% in the B2 phase. However, scatter between previous studies of the NaCl-B2 EoS (Heinz and Jeanloz 1984; Sata et al. 2002; Sato-Sorensen 1983; and unpublished data from our group) suggest that the NaCl-B2 volume can be affected by deviatoric stresses, even after laser annealing at high temperature. Therefore, such precision appears to be overestimated. In fact, the reproducibility of our experimental data suggest a precision of about 3% of the pressure, a value similar to that obtained using the ruby fluorescence technique. It is also compatible with the accuracy of the Pt EoS (see Holmes et al. 1989) that was used as a pressure standard to determine the NaCl-B2 EoS (Sata et al. 2002).

The uncertainties used in weighting the data in the least-squares fit of the EoS therefore represent our best estimates of the reproducibility of the experimental measurements. The resulting esd's of the parameters K_0 and K' derived from the least-squares matrix therefore only reflect the quality of fit to the data, or precision of the values. An estimate of the true uncertainty (i.e., accuracy) of the parameter values should also include the uncertainty in the pressure scale itself. Since all of our experimental pressure scales are linked to the ruby scale, and that is believed to have an absolute accuracy of about 0.3%, the additional uncertainty in the *accuracy* of K_0 is also 0.3%, or about an additional 1 GPa for stishovite. The influence of the pressure scale uncertainty on the value of K' depends on the form of the uncertainty. If the pressure scale is incorrect by a constant factor over the entire range of pressures, then this has no effect on the uncertainty of K'. But if the pressure scale has an inaccuracy that varies with pressure, the value of K' will be affected. With our current state of knowledge, this is impossible to evaluate.

Finite strain formalism

Analysis of compression data was done through the Eulerian finite-strain EoS. When truncated to the third order in energy, one obtains the Birch-Murnagham equation (Birch 1978):

$$P = 1.5\,K_0\,[(V_0/V)^{7/3} - (V_0/V)^{5/3}]\,\{1 + 0.75\,(K_0' - 4)\,[(V_0/V)^{2/3} - 1]\} \quad (1)$$

where K_0 and K_0' are the room pressure bulk modulus and its first pressure derivative, respectively. In Equation 1, the strain is defined relative to the strain state, and with the effective strain (f) and normalized stress (F),

$$f = 0.5\,[(V_0/V)^{2/3} - 1] \quad (2)$$

$$F = P / [3f(2f+1)^{5/2}] \quad (3)$$

Equation 1 transforms to

$$F = K_0\,[1 + 1.5\,f\,(K_0' - 4)] \quad (4)$$

F and f are provided by the experiments. K_0 and K_0' are the EoS parameters to be determined. The so-called f-F plot provides a useful visual representation of the EoS because the intercept of the experimental data on the F-axis (at $f = 0$) is the value of the bulk modulus at room pressure, and the experimental slope is a simple function of K_0'. Note that the f-F graph must be interpreted with caution, as the values of both f and F are dependent upon the value a priori chosen for V_0. Thus, the uncertainty of the V_0 value cannot be propagated to those of f and F. This is incompatible with experimental evidence that indicates that the uncertainties in the volume measurements at room pressure are comparable to those at high pressure. Therefore, K_0 and K_0' should be calculated directly from the BM3 equation (Eq. 1).

Stishovite equation of state

The stishovite EoS determined from the new single-crystal (Table 1) and powder-diffraction (Table 2) data are represented in Figure 2. The f-F plot (Fig. 3) shows that these two sets of data are very consistent with each other, at least for pressures up to ~60 GPa, before the transformation to the $CaCl_2$ form of SiO_2 occurs (Andrault et al. 1998; Kingma et al. 1995). In this plot, we note that the three data points that disagree most with the general trend (the EoS) are those corresponding to pres-

TABLE 1. Single-crystal data recorded in hydrostatic conditions

P	*a*	*b*	*V*
Amb.	4.17755(16)	2.66518(34)	46.5126(61)
1.168(6)	4.17119(27)	2.66356(30)	46.3429(53)
2.299(8)	4.16504(11)	2.66180(24)	46.1756(43)
3.137(8)	4.16051(14)	2.66062(29)	46.0550(51)
4.252(8)	4.15488(13)	2.65868(26)	45.8969(45)
5.037(11)	4.15084(15)	2.65767(30)	45.7902(53)
5.851(9)	4.14669(12)	2.65612(22)	45.6721(38)
6.613(8)	4.14323(14)	2.65470(27)	45.5715(50)
7.504(9)	4.13888(12)	2.65340(22)	45.4536(41)
8.264(11)	4.13555(15)	2.65226(30)	45.3609(56)
9.635(12)	4.12962(11)	2.64976(23)	45.1885(42)

Note: A single crystal of quartz is used as a pressure standard.

TABLE 2. Compression of stishovite embedded in NaCl pressure medium. The SiO_2 samples are laser-annealed after each compression step

P(GPa)	*V*(B1)	*V*(B2)	*a*	*b*	*V*
Amb.	179.818(13)				
11.69	138.538(12)		4.1217(1)	2.6458(1)	44.947(2)
17.67	128.833(21)		4.0962(1)	2.6381(1)	44.264(2)
22.38	122.42(22)	29.616(11)	4.0781(1)	2.6321(2)	43.776(3)
29.38	116.21(15)	28.283(14)	4.0552(3)	2.6192(5)	43.073(9)
37.71		26.163(10)	4.0287(3)	2.6048(4)	42.278(8)
46.03		25.055(12)	4.0035(4)	2.5919(10)	41.544(17)
52.73		24.290(11)	3.9859(4)	2.5806(4)	40.999(9)
26.32		28.088(5)	4.0576(2)	2.6217(3)	43.164(6)
30.98		27.229(2)	4.0440(2)	2.6155(3)	42.772(5)
34.21		26.695(1)	4.0308(1)	2.6101(2)	42.407(3)
38.45		26.056(2)	4.0207(2)	2.6037(2)	42.093(4)
43.37		25.388(1)	4.0030(2)	2.5966(2)	41.610(4)
47.49		24.880(2)	3.9907(3)	2.5921(4)	41.280(7)

Note: Pressures are calculated from volumes of the NaCl B2 or B1 forms, using EoS reported by (Brown 1999) and (Sata et al. 2002), respectively.

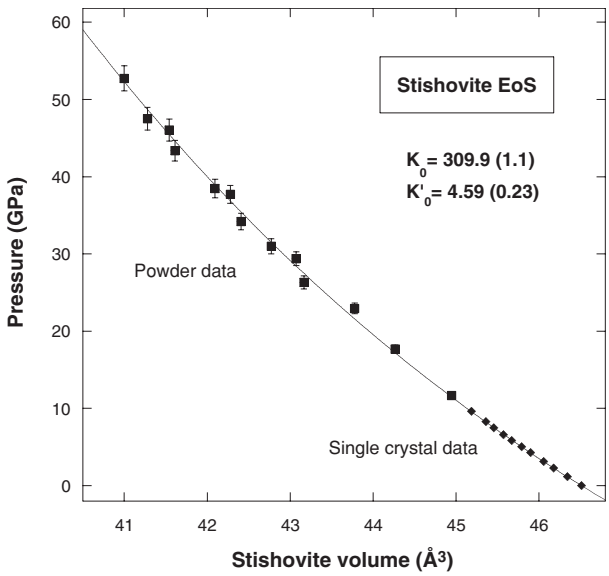

FIGURE 2. Compression curve of stishovite including the new single-crystal data using quartz as a pressure standard and powder diffraction data using NaCl as a pressure medium and pressure standard (see Table 1 and 2).

sures at which the NaCl B1 and B2 forms coexisted in the pressure chamber (see Table 2). Higher stresses were probably present in the pressure chamber due to the NaCl phase transformation. The positive slope of the *f-F* plot indicates that the value of K_0' is slightly greater than 4, a result that is not clear when the two data sets are considered separately. A refinement of a third-order Birch-Murnaghan EoS yields parameters of K_0 = 309.9(1.1) GPa and K_0' = 4.59(0.23). These new values deviate significantly from those obtained in our previous study, K_0 = 291 GPa and K_0' = 4]. As mentioned above, this is due to the previous use of an inaccurate Pt-EoS that underestimates the experimental pressures. The new results show stishovite to be even less compressible than previously reported. They are in reasonable agreement with the value of K_{0T} = 302(5) GPa obtained by ultrasonic interferometry (Li et al. 1996). The high value of *K*' is typical for rutile-structured oxides (e.g., Chang

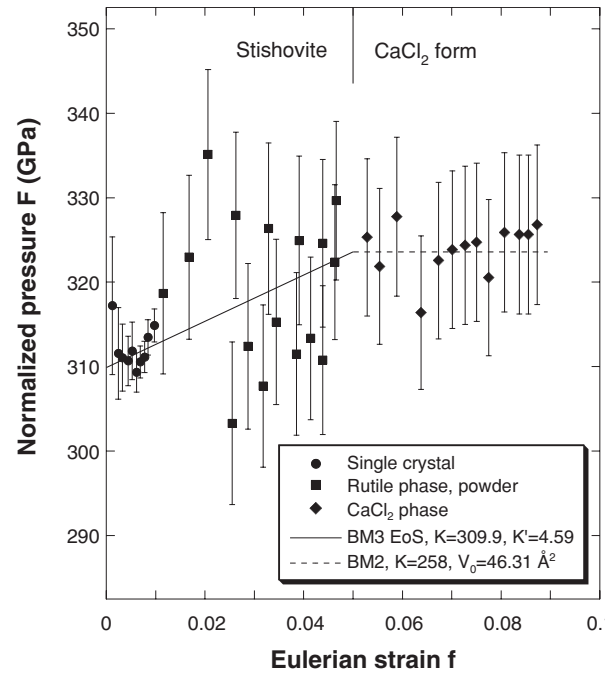

FIGURE 3. *F-f* plot (see equations 2 and 3) of SiO_2 data from our present and previous study (Andrault et al. 1998). For the latter set of data, we recalculated pressures using the Holmes et al. (1989) Pt-EoS. The positive slope in the *f-F* plot shows that the pressure derivative of the bulk modulus (K_0') is greater than 4 below the transition pressure to the $CaCl_2$ form of SiO_2.

and Graham 1975; Manghnani 1969; Wang and Simmons 1973).

The *a* (and *b*) axis of the tetragonal lattice of stishovite are found to be significantly more compressible than the *c* axis. A refinement of a second-order Birch-Murnagham EoS (with *K*' = 4) yields K_0 = 258(2) GPa or K_0 = 496(8) GPa for the pressure evolution of a^3 or c^3, respectively. The *c* parameter appears as a linear function of pressure up to 60 GPa. It contrasts with the pressure evolution of the *a* parameter, which exhibits significant curvature in this pressure range (Fig. 4). To model the pressure evolution of the stishovite lattice parameters, we thus use a third-order Birch-Murnagham EoS for a^3 [K_0 = 250.9(1.6) GPa and K_0' = 5.48(0.32)] and a linear equation for *c* ($c = 2.6654 - 0.001581\ P$).

PHASE TRANSITION IN SiO_2

Consistency between the different data sets

One aim of these new measurements was to clarify the nature of the phase transformation to the $CaCl_2$ polymorph, using all of the available data to the highest pressures. In particular, we wanted to make use of our previous data in which Pt was used as pressure standard (Andrault et al. 1998). But it is very important to prevent any systematic error that would result from misfits between the different data sets. For example, a slight inconsistency in pressure scales around the transition pressure can drive large errors in the calculation of spontaneous strains arising from the transition, and thus erroneous conclusions about the thermodynamic character of the transition. As the different

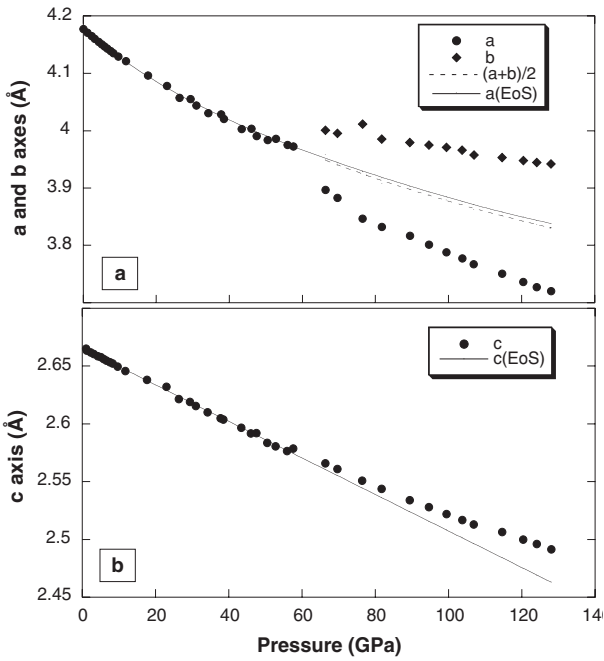

FIGURE 4. Pressure evolution of the SiO_2 unit-cell parameters in stishovite and $CaCl_2$ forms. (**a**) The evolution of *a* (circles) and *b* (diamonds) are reported together with the extrapolation of the *a* cell parameter of the stishovite (solid line), and a fit through the mean (*a* + *b*)/2 cell parameters of the $CaCl_2$ form (broken line). (**b**) The evolution of *c* (circles) is reported together with the extrapolation of the *c* cell parameter of the stishovite (solid line).

TABLE 3. Compression of SiO_2 without pressure medium

P (GPa)	*a*	*b*	*c*	*V*
50.47	3.9836(2)	3.9836(2)	2.5837(4)	41.000(8)
55.91	3.9755(3)	3.9755(3)	2.5767(8)	40.724(13)
57.56	3.9725(3)	3.9725(3)	2.5788(9)	40.695(15)
66.31	3.8971(7)	4.0008(8)	2.5658(2)	40.005(13)
69.58	3.8829(7)	3.9955(7)	2.5608(3)	39.729(13)
76.42	3.8467(11)	4.0114(12)	2.5509(4)	39.363(21)
81.72	3.8325(9)	3.9848(10)	2.5438(2)	38.848(16)
89.39	3.8170(10)	3.9787(11)	2.5339(2)	38.481(17)
94.64	3.8014(10)	3.9750(11)	2.5279(2)	38.198(17)
99.41	3.7882(9)	3.9709(10)	2.5221(2)	37.939(16)
103.7	3.7773(10)	3.9664(11)	2.5169(3)	37.709(17)
106.9	3.7675(6)	3.9576(7)	2.5130(2)	37.469(11)
114.6	3.7505(7)	3.9533(8)	2.5065(3)	37.164(13)
120.4	3.7364(7)	3.9482(8)	2.4998(2)	36.876(13)
124.1	3.7270(8)	3.9449(9)	2.4960(3)	36.699(13)
128.0	3.7201(8)	3.9422(9)	2.4913(3)	36.535(14)
Amb.	4.1803(2)	4.1803(2)	2.6635(7)	46.545(20)

Note: Data from Andrault et al. (1998). Above ~60 GPa the orthorhombic $CaCl_2$ form of SiO_2 is observed. Here, we recalculate pressures using the Pt EoS reported by Holmes et al. (1989).

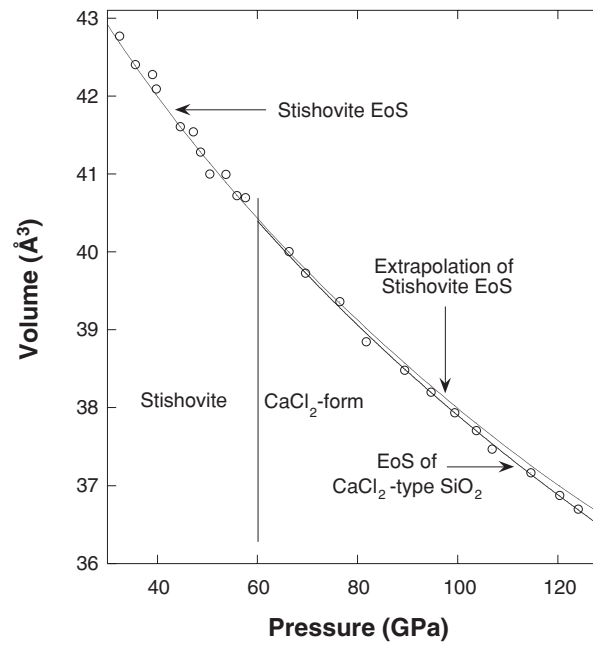

FIGURE 5. Compression curve of stishovite up to the highest pressures reached in our studies (Tables 2 and 3). The data points corresponding to the $CaCl_2$ structure-type plot slightly below the extrapolation of the stishovite EoS, showing that there is some volume strain associated with the phase transition.

Pt-EoS show significant scatter between one another, we found that the most secure procedure was to refine an apparent Pt bulk modulus for data points of our previous study. The refinement was done in two steps; first, the pressures corresponding to the previous data points recorded within the stishovite stability field were calculated from the volume and the newly determined stishovite EoS. Then, we used these pressures and the corresponding Pt-volumes to refine an apparent Pt bulk modulus. We obtained K_0 = 266.9 (3.6) GPa, with a first pressure derivative fixed to K_0' = 5.81. This is perfectly compatible with the EoS values of K_0 = 266 and K_0' = 5.81 reported by Holmes et al. (1989). We can thus conclude that the Pt did not encountered large differential stresses in our previous experiments. Also, we can safely use the Holmes EoS to derive pressures from the Pt volumes reported in our previous experiment (Table 3). Note that the Pt-EoS calculated here is significantly different than that reported by Jamieson et al. (1982).

EoS of the $CaCl_2$ phase

Combining the available data sets as described above, the SiO_2 compression curve and its corresponding *f-F* plot can then be drawn up to ~135 GPa (Figs. 3 and 5). A noticeable feature of the *f-F* plot is that the data for the $CaCl_2$ phase plot on a horizontal trend, slightly below the extrapolation of the stishovite EoS. This indicates that the K_0' value of the $CaCl_2$ phase is very close to 4, and that the $CaCl_2$ form becomes slightly more compressible than stishovite above the transition pressure. We obtain K_0 = 334(7) GPa and V_0 = 46.31(15) Å^3 for the $CaCl_2$ phase, with a first pressure derivative fixed to K_0' = 4. We refined a $CaCl_2$ form V_0 value slightly lower than that of stishovite, which seems contradictory with the slope of the compression curve, which is higher for the $CaCl_2$ form (Fig. 5). This effect is related to the greater value of K_0' for stishovite, which makes the curvature of its compression curve greater.

The pressure evolution of the *a*, *b*, and *c* unit-cell parameters of the $CaCl_2$ form are reported in Figure 4. Due to the symmetry breakdown from tetragonal to orthorhombic, the *a*

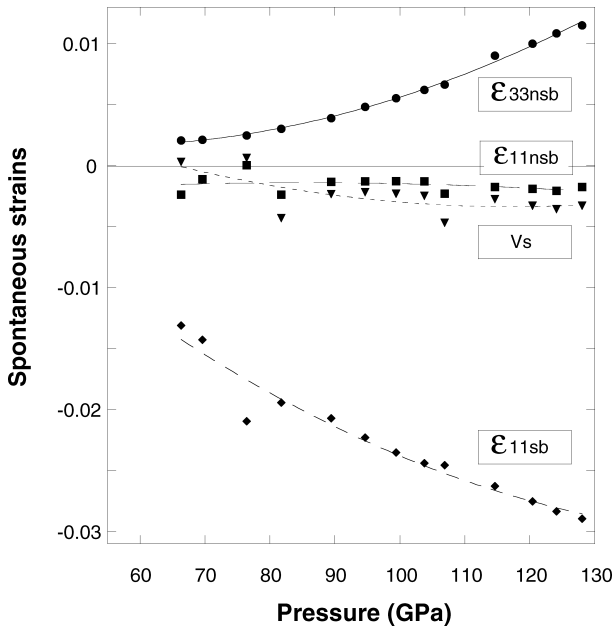

FIGURE 6. Symmetry-breaking (ε_{11sb}) and non symmetry-breaking (ε_{11nsb}, ε_{33}) spontaneous strains in the $CaCl_2$ form of SiO_2. The largest component appears to be $\varepsilon_{11sb,}$ in agreement with a mechanism of the phase transformation involving rotation of the SiO_6 octahedra in the *a*-*b* plane.

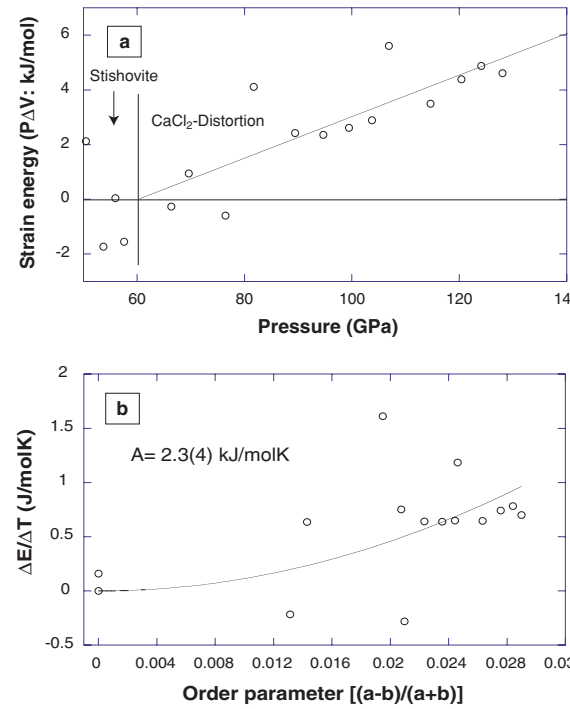

FIGURE 7. (**a**) Strain energy, as calculated from experimental volume strain and pressure (PΔV), plotted as a function of pressure. The energy strain increase continuously above the transition pressure, without any visible jump at 60 GPa. (**b**) The normalized energy ($\Delta E/\Delta T$, see text) shows a quadratic correlation with the order parameter, as expected for a purely second order transition in the Landau formalism truncated at second order ($\Delta E = -1/2A\Delta TQ^2$).

and *b* cell parameters diverge from the extrapolation of the stishovite *a* cell parameter above 60 GPa (as already reported by Andrault et al. 1998). In addition, we observe that the mean $CaCl_2$ form $(a + b)/2$ values plot at slightly lower value than the extrapolation of the *a* stishovite cell parameter. This contrasts with the behavior of the *c* axis parameter, which is found to be less compressible in the $CaCl_2$ form than in stishovite.

Spontaneous strains

The symmetry change at the phase transition is from the tetragonal rutile-structured phase to the orthorhombic $CaCl_2$ phase. The changes in lattice parameters that occur as the result of this transition (see Fig. 4) can therefore be expressed in terms of spontaneous strains, which in turn can be divided into "symmetry-breaking" and "non-symmetry-breaking" strains (e.g., Carpenter et al. 2000; Carpenter and Salje 1998). Specifically, the non-zero components of the symmetry-breaking strains are $\varepsilon_{11sb} = -\varepsilon_{22sb} = (a - b)/2a_0$, and the non-symmetry breaking strain components are $\varepsilon_{11nsb} = \varepsilon_{22nsb} = (a + b)/2a_0 - 1$ and $\varepsilon_{33nsb} = c/c_0 - 1$, where the subscripted cell parameters are those of the rutile-structured phase extrapolated to the pressures of the measurements of the $CaCl_2$ phase (Fig. 6). The two independent components of this non-symmetry-breaking strain, ε_{11nsb} and ε_{33nsb}, calculated from the extrapolations of the unit-cell parameters both remain small at all pressures, as does the volume strain $V_S = V/V_0 - 1$ derived from the extrapolation of the stishovite EoS. The fact that the relationship $2\varepsilon_{11nsb} + \varepsilon_{33nsb} = V_S$ is relatively preserved at all pressures indicates a reasonable level of uncertainty associated with the calculations of the spontaneous strain components. The largest component of spontaneous strain is clearly the symmetry-breaking strain, ε_{11sb}.

These trends are compatible with a transition mechanism that involves the rotation of the SiO_6 octahedra in the *a*-*b* plane. Indeed, if the main cause of this rotation is the occurrence of an O-O contact that becomes too short with increasing pressure (see Andrault et al. 1998), rather than the appearance of a new compression mechanism to reduce the volume, it seems logical that the symmetry-breaking strain component is the highest.

Landau analysis

The SiO_2 *P*-*V* plot shows that the volume of the $CaCl_2$ phase is smaller than the extrapolation of the EoS of stishovite above the phase transition at ~60 GPa (Fig. 5). The volume difference (ΔV) is much larger than the uncertainties associated with both the volume measurements and the extrapolation. The pressure difference is, however, of the same order as the error in the pressure determination (estimated to be ~3% in this pressure range). Still, the fact that all $CaCl_2$ data points plot below the extrapolation of the stishovite EoS above 80 GPa is a strong argument for a significantly denser $CaCl_2$ form in this high-pressure range. In contrast, previous analyses of the thermodynamics of the transition (Carpenter et al. 2000; Hemley et al. 2000) assumed that the non-symmetry breaking strains were negligible. At each pressure, the ΔV can be used to calculate

the energy difference ($\Delta E = P\Delta V$) between the two polymorphs. We observe that the strain energy (ΔE) increases progressively as a function of pressure above the transition pressure (Fig. 7a), a trend compatible with a second-order transition and a dominant symmetry-breaking strain component. The strain energy is found to be ~4 kJ/mole at ~120 GPa and 300 K. This value is significantly lower than, but of the same order of magnitude, as the enthalpy of fusion of SiO_2 quartz (9.4 kJ/mole) measured at room pressure (Richet et al. 1982).

Using the fact that the Clapeyron slope between stishovite and the $CaCl_2$ form is positive [P(GPa) = 51 + 0.012T(K); Ono et al. 2002], we propose to exchange pressure by temperature as the main parameter controlling the phase transformation. This is possible because the calculated strain energy, $\Delta E(P,300)$, related to the increase of pressure above the transition pressure at 300 K, can be compared with the thermal energy, $\Delta E(P_i, \Delta T)$, required to heat, at a given pressure (P_i), the sample from 300 K to the temperature of the Clapeyron slope. In fact, these energies are essentially equal if the heat capacity and the thermal expansion of the stishovite and $CaCl_2$ forms are similar. These assumptions are justified by the similarity between the two crystal structures. Therefore, each data point can be turned into a value of "thermal energy." [$\Delta E(P_i, \Delta T) = \Delta E = P\Delta V$] correlated with the Q order parameter, in a procedure similar to that for a typical Landau-analysis of a temperature-induced phase transformation. The order parameter of the transition is estimated as $Q = (a - b)/(a + b)$ to avoid the uncertainties, discussed above, associated with extrapolation of the unit-cell parameters of stishovite (Fig. 4). We observe that the normalized energy ($\Delta E/\Delta T$) plots as a quadratic function of the order parameter ($\Delta E = -1/2A\Delta TQ^2$), indicating that the phase transition is essentially second order (Fig. 7b).

ACKNOWLEDGMENTS

This paper is dedicated to Thomas Charpin. It is an IPGP and CNRS contribution.

REFERENCES CITED

Allan, D.R., Miletich, R., and Angel, R.J. (1996) A diamond-anvil cell for single-crystal X-ray diffraction studies to pressures in excess of 10 GPa. Review of Scientific Instruments, 67, 840–842.

Andrault, D. and Fiquet, G. (2001) Synchrotron radiation and laser-heating in a diamond anvil cell. Review of Scientific Instruments, 72, 1283–1288.

Andrault, D., Fiquet, G., Guyot, F., and Hanfland, M. (1998) Pressure-induced landau-type transition in stishovite. Science, 23, 720–724.

Angel, R.J. (2001) Equations of State. In R.M. Hazen, and R.T. Downs, Eds., High-pressure, high-temperature crystal chemistry, 41, p. 35–60. Reviews in Mineralogy and Geochemistry, Mineralogical of Society America, Washington, D.C.

Angel, R.J., Allan, D.R., Miletich, R., and Finger, L.W. (1997) The use of quartz as an internal pressure standard in high-pressure crystallography. Journal of Applied Crystallography, 30, 461–466.

Angel, R.J., Downs, R.T., and Finger, L.W. (2001a) Diffractometry. In R.M. Hazen, and R.T. Downs, Eds., High-pressure, high-temperature crystal chemistry, 41, p. 559–596. Reviews in Mineralogy and Geochemistry, Mineralogical of Society America, Washington, D.C.

Angel, R.J., Mosenfelder, J.L., and Shaw, C.S.J. (2001b) Anomalous compression and equation of state of coesite. Physics of the Earth and Planetary Interiors, 124, 71–79.

Birch, F. (1978) Finite strain isotherm and velocities for syngle crystal and pollycrystalline NaCl at high pressures and 300K. Journal of Geophysical Research, 83, 1257–1268.

Brown, J.M. (1999) The NaCl pressure standard. Journal of Applied Physics, 86, 5801–5808.

Carpenter, M.A. and Salje, E.K.H. (1998) Elastic anomalies in minerals due to structural phase transitions. European Journal of Mineralogy, 10, 693–812.

Carpenter, M.A., Hemley, R.J., and Mao, H.K. (2000) High-pressure elasticity of stishovite and the P4(2)/mnm reversible arrow Pnnm phase transition. Journal of Geophysical Research, 105, 10807–10816.

Chang, E. and Graham, E.K. (1975) The elastic constants of cassiterite SnO_2 and their pressure and temperature dependence. Journal of Geophysical Research, 80, 2595–2599.

Fiquet, G. and Andrault, D. (1999) Powder X-ray diffraction under extreme conditions of pressure and temperature. Journal of Synchrotron Radiation, 6, 81–86.

Heinz, D.L. and Jeanloz, R. (1984) Compression of the B2 high-pressure phase of NaCl. Physical Review B, 30, 6045–6050.

Hemley, R.J., Shu, J.F., Carpenter, M.A., Hu, J., Mao, H.K., and Kingma, K.J. (2000) Solid/order parameter coupling in the ferroelastic transition in dense SiO_2. Solid State Communications, 114, 527–532.

Holmes, N.C., Moriarty, J.A., Gathers, G.R., and Nellis, W.J. (1989) Equations of state of platinum to 660 GPa (6.6 Mbar). Journal of Applied Physics, 66, 2962–2967.

Jamieson, J.C., Fritz, J.N., and Manghnani, M.H. (1982) Pressure measurement at high temperature in x-ray diffraction studies: gold as a primary standard. In S. Akimoto, and M.H. Manghnani, Eds., High Pressure Research in Geophysics, p. 27–48. Riedel, Boston.

Jephcoat, A.P., Mao, H.K., and Bell, P.M. (1986) Compression of iron to 70 GPa with rare gas solids as pressure-transmitting media. Journal of Geophysical Research, 91, 4677–4684.

Kingma, K.J., Cohen, R.E., Hemley, R.J., and Mao, H.K. (1995) Transformation of stishovite to a denser phase at lower mantle pressures. Nature, 374, 243–245.

Larson, A.C. and Von Dreele, R.B. (1988) GSAS Manual. Report LAUR 86–748. Los Alamos National Laboratory.

Li, B.S., Rigden, S.M., and Liebermann, R.C. (1996) Elasticity of stishovite at high pressure. Physics of the Earth and Planetary Interiors, 96, 113–127.

Manghnani, M.H. (1969) Elastic constants of single-crystal rutile under pressures to 7.5 kilobars. Geophysical Research Letters, 1, 277–280.

Mao, H.K., Bell, P.M., Shaner, J.W., and Steinberg, D.J. (1978) Specific volume measurements of Cu, Mo, Pd, and Ag and calibration of the Ruby R_1 fluorescence pressure gauge from 0.06 to 1 Mbar. Journal of Applied Physics, 49, 3276–3283.

Mao, H.K., Xu, J., and Bell, P.M. (1986) Calibration of the ruby pressure gauge to 800 kbar under quasi-hydrostatic conditions. Journal of Geophysical Research, 91, 4673–4676.

McSkimmin, H.J., Andreatch, P., and Thurston, R.N. (1965) Elastic moduli of quartz versus hydrostatic pressure at 25 and -195.8°C. Journal of Applied Physics, 36, 1624–1633.

Ono, S., Hirose, K., Murakami, M., and Isshiki, M. (2002) Post-stishovite boundary in SiO_2 determined by in situ X-ray observations. Earth Planetary Science Letters, 6126, 1–6.

Orear, J. (1982) Least squares when both variables have uncertainties. American Journal of Physics, 50, 912–916.

Richet, P., Bottinga, Y., Denielou, L., Petitet, J.P., and Tequi, C. (1982) thermodynamic properties of quartz, cristobalite and amorphous SiO_2: drop calorimetry measurements between 1000 and 1800 K and a review from 0 to 2000 K. Geochimica et Cosmochimica Acta, 46, 2639–2658.

Ross, N.L., Shu, J.F., Hazen, R.M., and Gasparik, T. (1990) High pressure crystal chemistry of stishovite. American Mineralogist, 75, 739–747.

Sata, N., Shen, G., Rivers, M.L., and Sutton, S.R. (2002) Pressure-volume equation of state of the high-pressure B2 phase of NaCl. Physical Review B, 65, 114114–7.

Sato-Sorensen, Y. (1983) Phase transitions and equation of state for sodium halides: NaF, NaCl, NaBr, and NaI. Journal of Geophysical Research, 88, 3543–3548.

Wang, H. and Simmons, G. (1973) Elasticty of some mantle crystal structures 2. Rutile GeO_2. Journal of Geophysical Research, 78, 1262–1273.

MANUSCRIPT RECEIVED MARCH 22, 2002
MANUSCRIPT ACCEPTED NOVEMBER 13, 2002
MANUSCRIPT HANDLED BY YINGWEI FEI